ELSEVIER

Applied Surface Science 162–163 (2000) 1–8

applied surface science

www.elsevier.nl/locate/apsusc

Physical properties of cubic SiC(001) surfaces from first-principles simulations

Giulia Galli [a,*], Laurent Pizzagalli [a], Alessandra Catellani [b], Francois Gygi [a], Alexis Baratoff [c]

[a] *Lawrence Livermore National Laboratory, P.O. Box 808, Livermore, CA 94550, USA*
[b] *CNR–MASPEC, Parco Area delle Scienze, 37a, 43010 Parma, Italy*
[c] *Department of Physics and Astronomy, Basel University, Klingelbergstr. 82, CH-4056 Basel, Switzerland*

Abstract

We report the results of first-principles molecular dynamics simulations of the physical properties of cubic SiC(001) surfaces. In particular, we discuss the atomic geometries of several reconstructions, including (2×1), $c(4 \times 2)$ and (3×2), and compare computed STM images with recent experimental results. © 2000 Published by Elsevier Science B.V.

PACS: 73.20.At; 68.35.Bs
Keywords: Silicon carbide; Surface; Reconstruction; Ab-initio methods

1. Introduction

Silicon carbide is an attractive material for high-temperature micro- and optoelectronic devices [1] because of its wide band gap, high thermal conductivity, high hardness and chemical inertness. Having a small lattice mismatch with GaN, SiC has also emerged as a promising substrate for the growth of nitride-based devices [1,2].

In the last decade, a notable effort has been devoted to the characterization of SiC surfaces, since SiC films for use in technological applications are prepared by epitaxial growth. In particular, the (001) surfaces of the cubic polytype β-SiC have been studied with a variety of experimental [3–11] and theoretical [12–15] techniques. At the end of the 1980s, it was established that these surfaces are terminated by only one species and a clear assignment of different LEED patterns to either C- or Si-terminated surfaces was given [3]. Nevertheless, only very recently experimental and theoretical investigations have shed some light on the structural properties of the C- and Si-terminated surfaces, with many controversial issues about, e.g., SiC(001) surfaces with excess Si, remaining open. In this paper, we focus on the Si-terminated surface of SiC(001), for which a variety of reconstructions including (2×1), $c(4 \times 2)$ and $n \times 2)_{n=3,5,7\ldots}$ have been observed in LEED [3,16,17], RHEED [18] and STM [19–24] measurements.

Both (2×1) and $c(4 \times 2)$ reconstructions are believed to pertain to a complete Si monolayer at the

* Corresponding author.

0169-4332/00/$ - see front matter © 2000 Published by Elsevier Science B.V.
PII: S0169-4332(00)00162-8

top ($\theta_{Si} = 1$), as indicated by all available experimental data [17,18], although a controversial [25], theoretical paper [26] suggests a coverage of 1.5 for the c(4 × 2) reconstruction. It is now generally accepted that the reconstructions of SiC(001) are characterized by weakly bonded, flat dimers (p(2 × 1)) or by alternating symmetric dimers with different lengths (c(4 × 2)), unlike those of Si(001). The weak bonding character of Si–Si dimers is however in contradiction with the results of fits to LEED data, pointing at Si–Si dimers as tightly bound as on Si(001) surfaces [7].

The adsorption of additional Si atoms on the complete Si-terminated SiC(001) surface layer produces successive $(n \times 2)$ reconstructions as a function of Si coverage, including (7×2), (5×2), and a combination of (5×2) and (3×2) periodicities [17–19,21,23,24]. The (3×2) reconstruction seems to be the last stage before self-limitation of the growth [27]. Its atomic configuration and electronic structure are not clearly established, though they have been intensively investigated. In particular, theoretical investigations come to different conclusions [14,28], and discrepancies exist between different experimental probes [19–21,29,30].

Here, we summarize the results of several calculations on the p(2 × 1) [31,32], c(4 × 2) [31,32] and (3×2) [33] reconstructions, as obtained by performing first-principles molecular dynamics simulations both at zero and finite temperature, and by carrying out band-structure calculations for selected geometries. Our computations were done within Density Functional Theory, using the Local Density Approximation. We used pseudo-potentials and a plane wave basis set, which allowed us to perform systematic checks on the accuracy of computed quantities. In order to make contact with STM experiments, the tunneling current $I(x,y,z;V)$, and its derivative with respect to applied voltage V have been computed for selected, optimized geometries. The calculations have been carried out using the Tersoff–Hamman approximation [34], where $\partial I(x,y,z;V)/\partial V \propto \sum_i |\psi_i(x,y,z)|^2 \; f'(\epsilon_i + eV)$. Here, $\psi_i(x,y,z)$ and ϵ_i are single particle wavefunctions and eigenvalues, respectively, V indicates an applied voltage and f' is the derivative of the Fermi distribution. We refer the reader to the original papers for the details of our first-principles simulations.

2. Unstrained bulk: p(2 × 1) reconstruction

Given the apparent disagreement on the p(2 × 1) reconstruction of Si–SiC(001) between ab-initio calculations [15,31] and LEED measurements [7], we performed an extensive sampling of the potential energy surface in order to determine the most stable reconstruction. The potential energy of the system is extremely flat as surface atoms move in the plane parallel to the surface [15], and particular care must be taken in the sampling procedure. We first considered a slab with the periodicity of the unstrained bulk and therefore performed our calculations at the equilibrium theoretical lattice constant [31] of bulk SiC ($\alpha_{eq} = 4.30$ Å). We carried out total energy global optimizations starting from a series of different initial configurations. These include several c(4 × 2) geometries, with dimers having different lengths and buckling. We also devised starting configurations with symmetries lower than c(4 × 2). All of these configurations turned out to be unstable. Irrespective of the starting point of our calculations, we found the same stable minimum at the end of each optimization procedure. The most stable reconstruction is a weak p(2 × 1) pattern with unbuckled dimer rows (see Fig. 1a), having a total energy a few

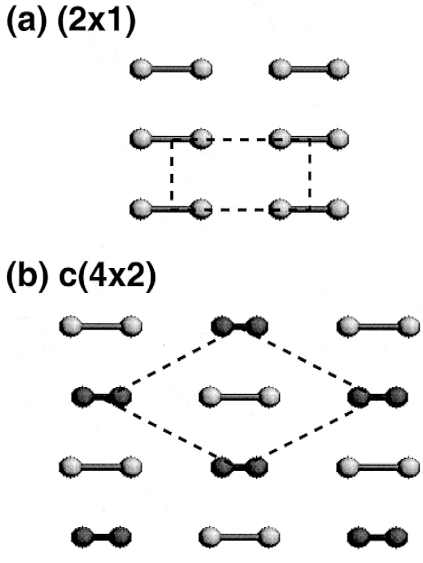

Fig. 1. Ball-and-stick representation of the p(2 × 1) (a) and c(4 × 2) (b) reconstructions of the (001) silicon-terminated surface of cubic SiC.

meV/atom lower than that of the ideal surface. The ideal surface corresponds to a metastable configuration. In our calculations we found that the surface symmetry is independent of the lateral supercell size used in the simulation, i.e. of the *k*-point sampling of the surface Brillouin zone (SBZ); on the contrary the dimer bond length varies from 2.58 to 2.63 Å when going from slabs with 8-atom to slabs with 16-atom per layer. The distances obtained in our calculations are much larger than the value deduced from fits of LEED patterns by Powers et al. [7]. These authors assumed a buckled dimer geometry, which might lead to errors in the resulting distances. Furthermore temperature [31] and stress effects (see below) could be responsible for reconstructions different from those observed at equilibrium.

We found that, similar to the ideal configuration, the $p(2\times1)$ reconstructed surface is non-metallic, with a gap between π^*-like and σ-like surface states. This is different from the electronic structure of the Si(001) and C(001) surfaces [35–37] where the reconstruction opens a band gap between π and π^* surface states.

Experimentally, the $p(2\times1)$ reconstructions of Si–SiC(001) have been often seen in areas of missing dimers [38] and low coverage [10]. It is, therefore, of interest to study a $p(2\times1)$ reconstructed surface with missing dimers, in order to analyze how these defects influence the reconstruction pattern. In our calculations, we found that the removal of a dimer induces the formation of stronger bonds in four dimers surrounding the missing unit; nevertheless it does not constitute a strong perturbation on the $p(2\times1)$ reconstruction, whose symmetry and dimer bond lengths are basically unchanged. We also found that removing a dimer lowers the surface tension considerably (by about 25% in our slab). Therefore we conclude that missing dimers allow the surface to relieve stress and thus help to stabilize the $p(2\times1)$ reconstruction.

3. Bulk under stress: $c(4\times2)$ reconstruction

Cubic SiC films are presently prepared by chemical vapor deposition on Si(001) substrates, the lattice mismatch between Si and SiC being almost 20%. This large mismatch is most probably accommodated within the interface layers by the formation of misfit dislocations. However the thermal mismatch (8%) between SiC and Si is responsible for residual stresses in SiC samples grown on Si, which are thus expected to be strained. It is, therefore, of interest to study the influence of stress on the surface reconstruction. When applying a uniaxial compressive stress along the Si dimers, we found that the symmetry of the surface is unchanged and the dimer bond length increases (2.75 Å) with respect to that of the unstrained bulk. This indicates that under uniaxial compressive stresses in the direction parallel to the dimers the surface tends to adopt an ideal geometry. On the contrary, when applying either a uniform tensile stress or a uniaxial tensile stress along the dimers, a change in the surface reconstruction is observed, in particular a symmetry breaking leading to a $c(4\times2)$ reconstruction. This is characterized by alternating unbuckled short and long dimers (see Fig. 1b), the short dimers having a smaller component in the direction perpendicular to the surface (z direction) than the long ones, by about 0.06 Å. The $c(4\times2)$ reconstruction found in our calculation is substantially different from that of Si(001) and is in very good agreement with the alternating-up-and-down dimer (AUDD) model recently proposed on the basis of STM experiments [24,38,39]. We would like to stress that the geometry found in our simulations is not inferred from comparisons of total energies for different fixed structures. It is the result of a spontaneous symmetry breaking of the potential energy surface, found in molecular dynamics simulations, which were performed in a supercell large enough to accommodate reconstructions with several different periodicities.

The surface states and the electronic structure of the $c(4\times2)$ surface are similar to those of the $p(2\times1)$. Close to the top of the valence band are two groups of four surface states with π character; these come from the small splitting of the bonding and antibonding states with π character, which takes place when the symmetry is lowered from $p(2\times1)$ to $c(4\times2)$ under tensile stress. Close to the conduction band bottom, we find surface states with σ character: these are atomic-like, non-bonding states. A difference between the electronic structures of the $p(2\times1)$ and $c(4\times2)$ reconstructions can be seen in the electronic density of states and could be detected

in photoemission experiments: below the Fermi level, the shoulder originating from surface states is more pronounced for the c(4 × 2) than for the p(2 × 1) reconstruction.

The computed STM images for the p(2 × 1) and c(4 × 2) reconstructions, at $V = -1.5$ eV, are reported in Fig. 2. The computed $\partial I(x,y,z_0;V)/\partial V$ is basically identical to the measured STM image at constant current [24,38]. Theoretically, states with large components on the dimers are observed in $\partial I/\partial V$ mode, while experimentally they are imaged in constant current mode: This might be related to a change in the energy difference between surface states induced by the tip electric field. Plots of $\partial I(x,y,z_0;V)/\partial V$ mainly show surface states with large components *on* the dimers. These are π-like bonding states. Bright spots appear on all dimers of the p(2 × 1) dimer rows (left); on the contrary only the up dimers are visible on the c(4 × 2) rows (right), in agreement with the recent experimental results of Ref. [24,38]. An isosurface of a Bloch state with π-like bonding character and large components on the dimers is reported in the left panel of Fig. 3, for the p(2 × 1) reconstruction. Plots of $I(x,y,z;V) = I_0$ show surface states having large components *between* dimers. These are bonding and antibonding π-like states. Depending on their position in the surface Brillouin Zone, both bonding and anti-bonding π-like Bloch states can have lobes tilted away from the dimers, overlapping with those of adjacent rows, since the distance between dimers is relatively small. Isosurfaces of two of these states are displayed in the middle and right panels of Fig. 3. States with maxima localized between dimers give

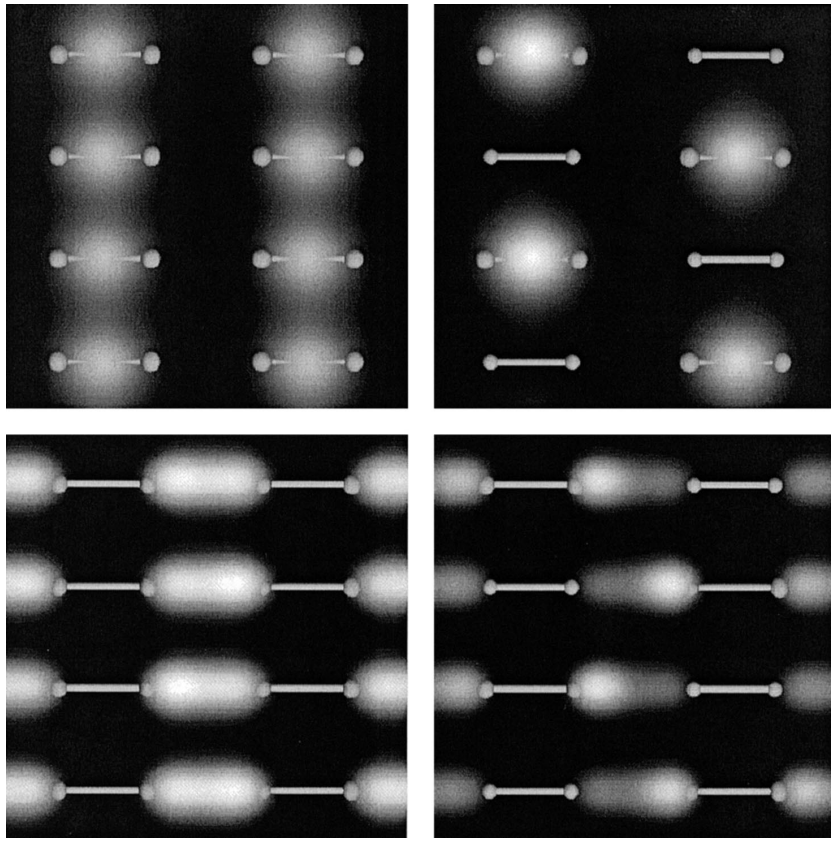

Fig. 2. Computed STM images of the p(2 × 1) (left panel) and c(4 × 2) (right panel) reconstructions of Si−SiC(001): the upper and lower panels show a plot of $\partial I(x,y,z_0;V)/\partial V \propto \sum_i |\psi_i(x,y,z_0)|^2 \; f'(\epsilon_i + eV)$ and $I(x,y,z;V) = I_0$, respectively (see text); in both cases $V = -1.5$ eV.

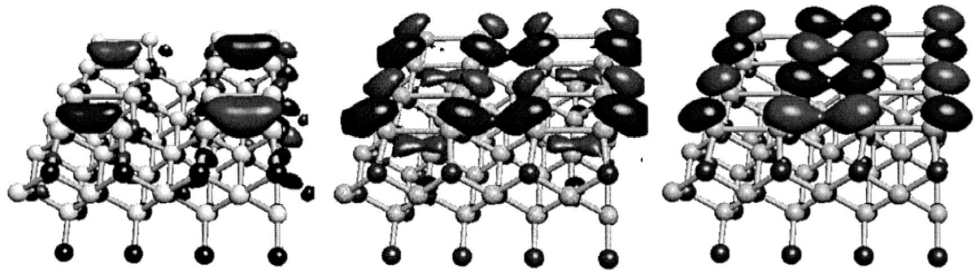

Fig. 3. Isosurfaces of selected surface states of the p(2×1) reconstruction of the (001) Si-terminated surface of cubic SiC, at different points of the surface Brillouin zone: the left and middle panels show bonding states at $k=(1,1)$ and $k=(0,1)$, respectively; the right panel displays an antibonding state at $k=(1,1)$.

rise to bright spots of $I(x,y,z;V)$ between dimers. On the p(2×1) surface these spots are identical on all dimers (Fig. 2, left), while on the c(4×2) surface (Fig. 2, right) they clearly show the difference in height between up and down dimers. This difference (Δz), as estimated from the comparison between experimental and computed STM images, is 0.1 Å [38,39], which is close to the value obtained in our work. Since the model used in Ref. [39] to estimate Δz is different from ours and since in our calculations we did not include the effect of the tip electric field on the sample, a quantitative comparison between experiment and our work is not straightforward.

4. Excess Si on Si−SiC(001): the (3×2) reconstruction

Three different atomic configurations, depicted on Fig. 4, have been suggested in the literature for the (3×2) reconstruction of Si−SiC(001). In the Double Dimer-Row (DDR) model, proposed by Dayan [16] and apparently supported by other experimental studies [19,24,29,30], there are two Si ad-dimers on top of the full Si layer (Fig. 4a). The resulting coverage $\theta_{Si}=2/3$ is in contradiction with the measured θ_{Si} value of $1/3$ claimed by several groups [17,18,27]. The straightforward extension of this model to the (5×2) reconstruction is also inconsistent with the measured coverage [18]. Moreover, this model is not supported by some STM studies [20,21]. Another model, ADDed dimer-row (ADD), was first suggested in an early study by Hara et al. [17]. This configuration, with one Si ad-dimer per unit cell (Fig. 4b), corresponds to the measured coverage for the (3×2) and (5×2) reconstructions. However, though it appears consistent with several experimental data, both empirical [40] and ab-initio [14] calculations have shown that it is not energetically favored. Furthermore, STM investigations do not support this model [19,20]. Another $1/3$ coverage model, the ALTernate dimer-row (ALT), was proposed by Yan et al. [14].This configuration is supported both by calculations [14,40] and by STM studies [20,21]. However, it cannot account for the observed relation between single domain LEED patterns with (2×1) and (3×2) periodicities [3,41]. It also fails to explain the (3×1) reconstruction observed after O or H adsorption [16,19]. Note that all three models involve Si ad-dimers, which are perpendicular to the dimers on the underlying Si surface. Indeed, previous calculations have shown that a single parallel ad-dimer is energetically much less favored than a perpendicular one [42].

The relaxed atomic structures computed for the three models are shown on Fig. 4. In the DDR geometry, one ad-dimer is strongly tilted ($\delta z=0.62$ Å) and has a short bond length ($d=2.26$ Å) while the other, weakly bound ($d=2.66$ Å), is almost flat ($\delta z=0.03$ Å). The inequivalence of the two ad-dimers disagrees with simple expectations [16,19] and with previous calculations by Kitabatake and Greene [28], who found two flat ad-dimers for the DDR model. A single flat and weakly bonded ad-dimer ($d=2.62$ Å) is obtained in the ADD model, the geometry being close to that previously obtained by Yan et al. [14] in a calculation similar to ours.

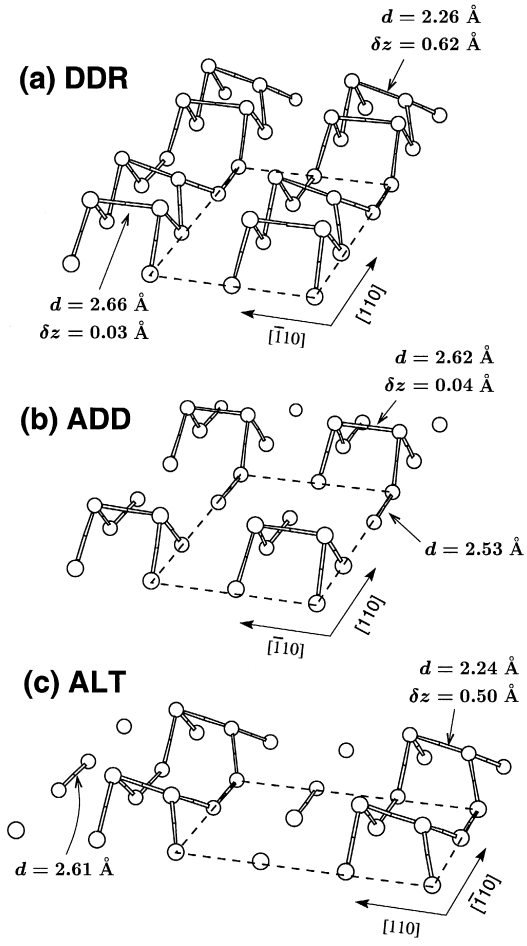

Fig. 4. Ball-and-stick representation of the relaxed atomic structures for the DDR (a), ADD (b), and ALT (c) models of the (3×2) reconstructed surface of SiC(001). d and δz are the distance and height difference between adatoms, respectively. Only the ad-layer and the first underlying Si layer are shown for clarity.

Finally, in the ALT model, the ad-dimer is strongly tilted ($\delta z = 0.5$ Å) and strongly bound ($d = 2.24$ Å), in good agreement with previous calculations [14]. The length of the weak Si dimers in the underlying surface layer is close to the value computed for the (2×1) reconstruction.

The total energy comparison of the three models of Fig. 4 is not straightforward owing to their different numbers of adatoms. This difficulty can be overcome by using the grand canonical scheme [43]. We found that the ALT model is the most stable configuration over the entire allowed range of the Si chemical potential. However, the energy difference between ALT and DDR obtained under Si-rich conditions is only 77 meV, i.e. within our error bar.

Several experimental STM studies of the (3×2) reconstruction are currently available [19,20,44,45]. In order to make contact with these experiments, filled states constant-current STM images of the three models of Fig. 4 have been calculated. Representative images are shown in Fig. 5. In both the DDR and ADD models, we find strings of peanut-shaped spots, originating from a slight overlap between maxima on adjacent flat ad-dimers. For the DDR model, additional maxima are located on the up adatoms of the tilted ad-dimers. The resulting images are incompatible with the experimental observations of a single oval spot stretched in the [110] direction per 3×2 cell. On the other hand, in the

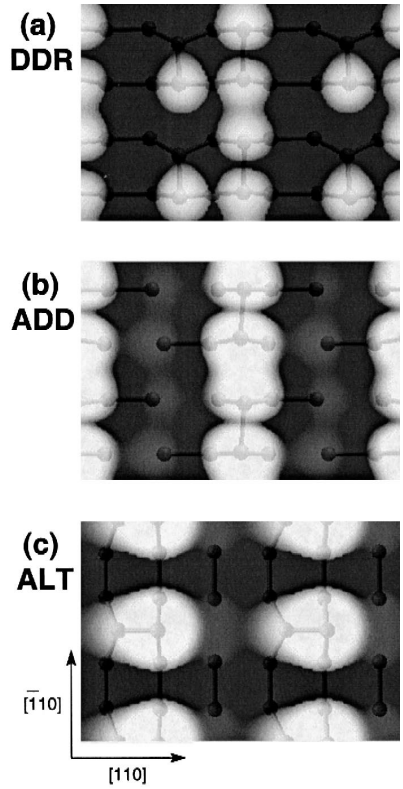

Fig. 5. Calculated constant-current STM images (bias $V = -1$ V) for the DDR (a), ADD (b), and ALT (c) models of the (3×2) reconstructed surface of SiC(001).

ALT model, the spread-out stretched spots located above up adatoms of the tilted ad-dimers are in accord with experimental STM images of filled states [20].

Additional insight into the electronic structure of the (3×2) reconstructed surface can be obtained from analyses of the electronic states within a few eV of the Fermi level. All photoemission measurements agree about the presence of two occupied surface states in the band gap, 1 eV apart from each other [30,46,47]. However, uncertainties exist about the location of these states with respect to the Valence Band Maximum (VBM). Recent angle-resolved photoemission spectroscopy (ARPES) measurements have shown that the dispersion of all identified surface states is very small (≤ 0.2 eV) along the $[\bar{1}10]$ [30] and [110] [30,47] directions. Only the surface states of the DDR and ALT models have been considered in our calculations, the ADD model being higher in energy than the ALT model and exhibiting STM images which do not agree with experiment.

We find that in the DDR model the surface is metallic, within the Local Density Approximation. The highest occupied state, about 1 eV above the VBM at Γ, is mainly localized on the flat ad-dimer and has a π^* character with respect to the dimer axis. Its dispersion is very small along the [110] direction (≤ 0.1 eV), but rather strong along the $[\bar{1}10]$ direction ($\simeq 1$ eV). In the DDR model, we also find three additional surface states with energies between the highest occupied state and the VBM. Only one of them is localized above the up adatom of the tilted ad-dimer, and is essentially dispersionless. The other two states originate from backbond and dimer states of the underlying surface, and show strong dispersions. The presence of dispersive states in the band gap is in disagreement with ARPES evidence and points against the DDR model.

In the ALT model, the surface is semiconducting, with a direct gap at Γ of about 0.5 eV. The highest occupied state, 0.8 eV above the VBM at Γ, is localized on the up adatom of the tilted ad-dimer and has a strong 's' character. This surface state has a small dispersion along both [110] and $[\bar{1}10]$ directions (≤ 0.1 eV). Close to the VBM we find another state, lying 0.7 eV below the highest occupied orbital. It is a π^* state localized on the Si–Si dimer of the underlying surface which are not bonded to ad-dimers, and is nearly dispersionless (≤ 0.2 eV). This state is only present in the [110] direction. Except for the energy difference between the two highest surface states (0.7 vs. 1 eV), agreement with ARPES experiments is definitely better for the ALT than the DDR model.

5. Conclusion

In summary, we have studied the physical properties of reconstructed Si–SiC(001) surfaces. Our calculations have shown that an unstrained bulk exhibits a non-metallic $p(2\times1)$ reconstruction. Missing dimers allow the surface to relieve stress and help stabilize this reconstruction. Small applied stresses were found to lower the symmetry of the surface reconstruction from $p(2\times1)$ to $c(4\times2)$. This suggests that residual stresses in SiC grown on Si are responsible for the different reconstruction patterns observed experimentally. Calculated STM images are in excellent agreement with experimental results. We have also performed a comparative study of three different models for the (3×2) reconstruction associated with excess Si on the surface. Our calculations strongly favor one of the models, and exclude the two others, although some ambiguities remain. More decisive conclusions on this reconstruction could come from an experimental confirmation of the Si coverage corresponding to the (3×2) reconstruction.

Acknowledgements

This work was supported by (i) the US Department of Energy, Office of Basic Energy Sciences, Division of Materials Science, Contract No. W-7405-ENG-48; (ii) the Swiss National Foundation program NFP36 and the Swiss Center for Scientific Computing; (iii) the Italian ''Consiglio Nazionale delle Ricerche''.

References

[1] H. Morkoç, S. Strite, G.B. Gao, M.E. Lin, B. Sverdlov, M. Burns, J. Appl. Phys. 76 (1994) 1363.
[2] R. Dupuis (Ed.), Proceeding of the 1995 MRS Fall Meeting: Gallium Nitride and Related Materials, 1996.

[3] R. Kaplan et al., Surf. Sci. 215 (1989) 111.
[4] V. Bermudez, R. Kaplan, Phys. Rev. B 44 (1991) 11149.
[5] J. Powers, A. Wander, P.J. Rous, M.A. Van Hove, G.A. Somorjai, Phys. Rev. B 44 (1991) 11159.
[6] T. Parrill, Y. Chung, Surf. Sci. 243 (1991) 96.
[7] J. Powers, A. Wander, M.A. Van Hove, G.A. Somorjai, Surf. Sci. Lett. 260 (1992) L7.
[8] V. Bermudez, J. Long, Appl. Phys. Lett. 66 (1995) 475.
[9] F. Semond, P. Soukiassian, P.S. Mangat, L. di Cioccio, J. Vac. Sci. Technol., B 13 (1995) 1591.
[10] M. Shek, Surf. Sci. 349 (1996) 317.
[11] J. Long, V. Bermudez, D. Ramaker, Phys. Rev. Lett. 76 (1996) 991.
[12] B. Craig, P. Smith, Surf. Sci. Lett. 256 (1991) L609.
[13] P. Badziag, Phys. Rev. B 44 (1991) 11143.
[14] H. Yan, A. Smith, H. Jónsson, Surf. Sci. 330 (1995) 265.
[15] M. Sabisch, P. Krüger, A. Mazur, M. Rohling, J. Pollmann, Phys. Rev. B 53 (1996) 13121.
[16] M. Dayan, J. Vac. Sci. Technol., A 4 (1985) 38.
[17] S. Hara et al., Surf. Sci. Lett. 231 (1990) L196.
[18] T. Yoshinobu et al., Appl. Phys. Lett. 59 (1991) 2844.
[19] S. Hara, S. Misawa, S. Yoshida, Y. Aoyagi, Phys. Rev. B 50 (1994) 4548.
[20] F. Semond et al., Phys. Rev. Lett. 77 (1996) 2013.
[21] P. Soukiassian, F. Semond, A. Mayne, G. Dujardin, Phys. Rev. Lett. 79 (1997) 2498.
[22] V.Y. Aristov, L. Douillard, O. Fauchoux, P. Soukiassian, Phys. Rev. Lett. 79 (1997) 3700.
[23] L. Douillard, V.Y. Aristov, F. Semond, P. Soukiassian, Surf. Sci. Lett. 401 (1998) L395.
[24] J. Kitamura et al., unpublished.
[25] P. Soukiassian, V.Yu. Aristov, L. Douillard, F. Semond, A. Mayne, G. Dujardin, L. Pizzagalli, C. Joachim, B. Delley, E. Wimmer, Phys. Rev. Lett. 82 (1999) 3721.
[26] W. Lu, P. Krüger, J. Pollmann, Phys. Rev. Lett. 81 (1998) 2292.
[27] S. Hara et al., Surf. Sci. 273 (1992) 437.
[28] M. Kitabatake, J.E. Greene, Appl. Phys. Lett. 69 (1996) 2048.
[29] H.W. Yeom et al., Phys. Rev. B 56 (1997) R15525.
[30] H.W. Yeom et al., Phys. Rev. B 58 (1998) 10540.
[31] A. Catellani, G. Galli, F. Gygi, Phys. Rev. Lett. 77 (1996) 5090.
[32] A. Catellani, G. Galli, F. Gygi, Phys. Rev. B 57 (1998) 12255.
[33] L. Pizzagalli, A. Catellani, G. Galli, F. Gygi, A. Baratoff, Phys. Rev. B 60 (1999) R5129.
[34] J. Tersoff, D. Hamann, Phys. Rev. B 31 (1985) 805.
[35] A. Ramstad, G. Brocks, P. Kelly, Phys. Rev. B 51 (1995) 14504.
[36] J. Furthmueller, G. Kresse, Phys. Rev. B 53 (1996) 7334.
[37] P. Krüger, J. Pollmann, Phys. Rev. Lett. 74 (1995) 1155.
[38] P. Soukiassian, F. Semond, G. Dujardin, A. Mayne, L. Douillard, L. Pizzagalli, C. Joachim, Phys. Rev. Lett. 78 (1997) 907.
[39] L. Pizzagalli, C. Joachim, A. Mayne, G. Dujardin, F. Semond, L. Douillard, P. Soukiassian, Thin Solid Films 318 (1998) 136.
[40] H. Yan, X. Hu, H. Jónsson, Surf. Sci. 316 (1994) 181.
[41] V.M. Bermudez, Phys. Status Solidi B 202 (1997) 447.
[42] A. Catellani, G. Galli, F. Gygi, Appl. Phys. Lett. 72 (1998) 1902.
[43] G.-X. Qian, R.M. Martin, D.J. Chadi, Phys. Rev. B 38 (1988) 7649.
[44] S. Hara et al., Surf. Sci. 357–358 (1996) 436.
[45] S. Hara et al., Surf. Sci. 421 (1999) L143.
[46] M.L. Shek et al., J. Vac. Sci. Technol., A 12 (1994) 1079.
[47] M. Lübbe et al., J. Vac. Sci. Technol., A 16 (1998) 3471.